THESIS FOR THE DEGREE OF LICENTIATE OF ENGINEERING

Proton conducting ionic liquids

Binary mixtures and structural modifications

Iqbaal Abdurrokhman

Department of Chemistry and Chemical Engineering
CHALMERS UNIVERSITY OF TECHNOLOGY

Gothenburg, Sweden 2020

Proton conducting ionic liquids
Binary mixtures and structural modifications
IQBAAL ABDURROKHMAN

Licentiatuppsatser vid Institutionen för kemi och kemiteknik
Chalmers tekniska högskola
Nr 2020:07

Department of Chemistry and Chemical Engineering
Chalmers University of Technology
SE-412 96 Gothenburg
Sweden
Telephone: +46 (0)31-772 1000

Cover
A cartoon representing the challenge of finding suitable ionic liquids for proton exchange membrane fuel cell applications. Art by Eka Susanti.

Printed by Chalmers Reproservice
Gothenburg, Sweden 2020

Proton conducting ionic liquids
Binary mixtures and structural modifications

Iqbaal Abdurrokhman

Department of Chemistry and Chemical Engineering
Chalmers University of Technology

Abstract

Proton conduction is a phenomenon of fundamental importance for biological and chemical systems, such as in photosynthesis and aerobic respiration. Proton conduction is also key in the proton exchange membrane fuel cell, a clean electrochemical device that converts chemical into electrical energy. The archetypical proton exchange membrane is currently a perfluorinated polymer with pending acidic groups. The fuel cell technology is presently at renewed focus in the commercial sector, and consequently also in the scope of research and development programs. In order to enable the development of more sustainable proton exchange membrane fuel cells, new requirements have been set that for instance target operation at higher temperatures and anhydrous conditions. In this context, protic ionic liquids have been highlighted as interesting next-generation electrolytes with the potential to assist proton conduction. Protic ionic liquids are a subset of ionic liquids, also known as low temperature molten salts, entirely composed of ions and displaying very low vapor pressures. Moreover, a protic ionic liquid has an exchangeable proton and is able to establish extended networks of hydrogen bonds. Understanding the dynamics of this local structures is fundamental to design new protic ionic liquids able to sustain a fast proton motion decoupled from the diffusion of the ionic species. To achieve such a dynamical behavior we have investigated two different approaches, that is i) mixing a protic ionic liquid candidate with a co-solvent (here ethylene glycol) able to participate in the hydrogen bonds and ii) modifying the molecular structure of the cation (here by alkyl chains of length (n) varying from ethyl (n=2) to dodecyl (n=12)) in a series of imidazolium based protic ionic liquids. The local intermolecular interactions, the nano-structuration as well as ionic and protonic dynamics have been investigated by suitable techniques that include vibrational spectroscopy, NMR spectroscopy, diffusion NMR, impedance spectroscopy and X-ray scattering.

Keywords: Protic ionic liquids, fuel cell, hydrogen bonds, nanostructure

Acknowledgements

The research was performed at the Division of Applied Chemistry in the Department of Chemistry and Chemical Engineering, in part also at the Chalmers Materials Analysis Laboratory and at the Swedish NMR Centre in Gothenburg. This work has been performed with the funding support from Knut & Alice Wallenberg Foundation.

First and foremost, I would to like express my gratitude to my supervisor Assoc. Prof. Anna Martinelli for giving me the opportunity to work and dive in protic ionic liquids world, thank you for the understanding and time whenever I need moral or scientific support. Special thanks to Prof. Jan Swenson for allowing me to learn the beauty of broadband dielectric spectroscopy, my examiner Prof. Per-Anders Carlsson, and the Director of studies Prof. Lars Nordstierna.

My gratitude goes to all collaborators in the first and second paper in this thesis.

I am really grateful to all members of Anna Martinelli's research group, Khalid, Mohammad, Olesia, Szilvia and Eduardo.

Thank to present and previous colleagues at the division of Applied Chemistry for the positive and enjoyable working environment.

I also thank my former supervisor Prof. Lee Ming-Jer at the National Taiwan University of Science and Technology (NTUST), without your introduction to the world of ionic liquids, I would not be where I am today. Also thank to all previous members in E-504 and *Teknik Reaksi Kimia* laboratory, its been a pleasure to know you all.

I would like to thank all indonesian friends in Gothenburg. I could not mention all of you but I do appreciate your help during my stay in Gothenburg.

Finally, of course, I thank my family in Indonesia and my girlfriend for all the prayer, love and support you gave to me. Terimakasih banyak doa-doa nya selama saya disini.

Iqbaal Abdurrokhman
Gothenburg, May 2020

List of publications

This thesis is based on the following appended papers:

I. Transport properties and intermolecular interactions in binary mixtures based on the protic ionic liquid ethylimidazolium triflate and ethylene glycol
Negin Yaghini, Iqbaal Abdurrokhman, Mohammad Hasani and Anna Martinelli
Physical Chemistry Chemical Physics, ***2018****, 20, 22980-22986*

II. Protic Ionic Liquids Based on the Alkyl-Imidazolium Cation: Effect of the Alkyl Chain Length on Structure and Dynamics
Iqbaal Abdurrokhman, Khalid Elamin, Olesia Danyliv, Mohammad Hasani, Jan Swenson and Anna Martinelli
Journal of Physical Chemistry B, ***2019****, 123, 4044-4054*

My contribution to the publications:

Paper I
Responsible for collecting and analysing vibrational spectra (Raman and infrared). Together with the other authors discussed all the results and contributed to finalising the whole work.

Paper II
Responsible for most of the experimental work (except X-ray and diffusion experiment), data analysis, and writing of the first draft of the manuscript.

List of figures

Figure:

2.1 Walden plot for ionic liquids with various cations showing a behavior below the KCl ideal line 7
2.2 Synthesis routes used to obtain protic and aprotic ionic liquids . . 8
2.3 Illustration of various proton transport mechanisms, vehicular mechanism in [C_2HIm][TFSI] and Grotthuss mechanism in water 13

3.1 The typical plot of thermogravimetric analysis result, here for the sample [C_2HIm][TFSI] 16
3.2 Example of typical DSC curve of a protic ionic liquid. The sample was cooled fast and followed by subsequent heating at a rate of 5 K·min^{-1}. 17
3.3 Infrared spectroscopy sketch and typical graph result 19
3.4 General schematic for a) Raman spectroscopy and b) Scattering types : Stokes, Rayleigh, Anti-Stokes 20
3.5 Schematic illustration on small angle X-ray scattering working principle 21
3.6 A simple representation of a fluid placed between two parallel plates in cartesian coordinate 23
3.7 Schematic figure for: a) Broadband dielectric spectroscopy measurement, and b) The broadband dielectric spectroscopy cell used in this thesis 24
3.8 Spin states of proton in the presence of external magnetic field (B_0) 24

4.1 Thermal stability comparison for selected system, [C_2HIm][TfO]-ethylene glycol at 0.5 mole fraction of ethylene glycol and neat [C_2HIm][TFSI] 27
4.2 High frequency region of infrared spectra of a) [C_2HIm][TfO]-ethylene glycol mixtures, b) [C_nHIm][TFSI] series; and Raman wavenumber of c) S-O stretching mode for [C_2HIm][TfO]-ethylene glycol mixtures as a function of ethylene glycol mole fraction, d) Symmetric bending modes of CF_3 for [C_nHIm][TFSI] series as a function of n 28
4.3 Wide angle X-ray scattering recorded spectra and analysis results for the [HC_nIm][TFSI] series, n from 2 to 12 29

4.4 Proposed illustration of the possible H-bonds interactions in protic ionic liquid-ethylene glycol mixtures 30
4.5 a) ^{1}H NMR results of [HC_nIm][TFSI] protic ionic liquids as a function of alkyl chain length, dashed line are simply guide to the eye; b) D_{NH}/D_{cation} ratio results of [C_2HIm][TfO]-ethylene glycol mixture and [HC_nIm][TFSI], varying n from 2 to 12 31
4.6 Ionic conductivity results of a) [C_2HIm][TfO]-ethylene glycol mixture and b) [HC_nIm][TFSI] protic ionic liquids, with n from 2 to 12. The dash line is simply a guide to the eye 32

List of abbreviation and symbols

AIL	Aprotic Ionic Liquid
BDS	Broadband Dielectric Spectroscopy
DSC	Differential Scanning Calorimetry
FC	Fuel Cell
HC_nIm	1H-3-Alkyl-imidazolium
IL	Ionic Liquid
NMR	Nuclear Magnetic Resonance
PEMFC	Proton Exchange Membrane Fuel Cell
PFG NMR	Pulsed Field Gradient Nuclear Magnetic-Resonance
PIL	Protic Ionic Liquid
TfO	Triflate
TFSI	Bis(trifluoromethylsulfonyl)imide
TGA	Thermogravimetric Analysis
δ	Gradient pulse duration
Δ	Self-diffusion time
D	Self-diffusion coefficient
η	Viscosity
λ	Laser wavelength
n	Alkyl chain length
σ	Ionic conductivity
T_c	Crystallisation Temperature
T_d	Decomposition Temperature
T_g	Glass Transition Temperature
T_m	Melting Temperature

Contents

Abstract iii

Acknowledgements v

List of publications vii

List of figures ix

List of abbreviation and symbols xi

Contents xiii

1 Introduction 1
- 1.1 General scientific context . . . 1
  - 1.1.1 The proton exchange membrane fuel cell: requirements and challenges . . . 1
  - 1.1.2 Electrolyte materials . . . 2
- 1.2 Objectives of this work . . . 3
- 1.3 Organization of this thesis . . . 4

2 Ionic liquids 5
- 2.1 History . . . 5
- 2.2 Classes of ionic liquids . . . 6
- 2.3 Protic ionic liquids . . . 6
- 2.4 Synthesis . . . 7
- 2.5 Properties of ionic liquids . . . 8
  - 2.5.1 Thermal stability . . . 9
  - 2.5.2 Molecular interactions . . . 9
  - 2.5.3 Nanostructure . . . 10
  - 2.5.4 Transport properties . . . 11

3 Experimental methods and procedures 15
- 3.1 Thermal analyses . . . 15
  - 3.1.1 Thermogravimetric analysis (TGA) . . . 15
  - 3.1.2 Differential scanning calorimetry (DSC) . . . 16
- 3.2 Vibrational spectroscopy . . . 18
  - 3.2.1 Infrared spectroscopy . . . 18

3.2.2 Raman spectroscopy 19
3.3 X-ray scattering 20
3.4 Transport properties 21
3.4.1 Density 21
3.4.2 Viscosity 22
3.4.3 Ionic conductivity 23
3.4.4 NMR spectroscopy 24

4 Results and discussion **27**
4.1 Thermal stability 27
4.2 Intermolecular interactions 28
4.3 Nanostructuration 29
4.4 Ionic mobility 31
4.5 Ionic conductivity 32

5 Conclusions and outlook **35**

References **37**

Appended papers **43**

Paper I **45**

Paper II **57**

1 Introduction

1.1 General scientific context

In 1914, Paul von Walden published a paper on a low melting temperature salt obtained from the neutralisation of ethylamine with nitric acid. Initially, this work did not receive a major interest from other scientists. Today, about a century after this discovery, this material is one of the most known and studied ionic liquids (ILs). A significant amount of scientific articles on ionic liquids have been published since then, covering a vast number of applications such as separation processes, lubrification, metal extraction, catalysis and electrochemistry [1–6]. This chapter presents a specific context in which ionic liquids are relevant, the fuel cell. By describing briefly the requirements and challenges related to next-generation fuel cells, the motivation of my work is also put at place.

1.1.1 The proton exchange membrane fuel cell: requirements and challenges

Energy conversion from petroleum, natural gas, coal, or fossil fuels create emissions that affect the environment. Our reliance on fossil fuels in many sectors such as transportation, heat generation and electricity creates major problems on our environment, *e.g.* air pollution and global climate [7, 8]. Therefore, better energy devices that convert fuel into energy with less pollution are required. There are several types of energy relevant devices of societal interest, such as wind turbines, solar cells, organic batteries, supercapacitors, and fuel cells [9].

The fuel cell (FC) is very promising technology because it converts chemical energy directly into electricity with water being the only product (undesirable pollutants such NO_x, SO_x are zero) and does not rely on moving parts. Currently, there are different types of fuel cells, for example the solid oxide fuel cell (SOFC), the phosphoric acid fuel cell (PAFC), the alkaline fuel cell (AFC), the molten carbonate fuel cell (MCFC) and the proton exchange membrane fuel cell (PEMFC) [10].

The PEMFC is promising for heavy duty or large scale applications since it can provide high power density, large energy capacity, and high efficiency; moreover it can use different energy sources like hydrogen, methanol, or ethanol [11, 12]. The electrochemical half reactions that occur in a PEMFC are written in equation 1.1, with oxidation of hydrogen occurring at the anode and reduction of oxygen

occurring at the cathode [10].

$$\mathrm{H_2} \longrightarrow \mathrm{H^+} + 2\,\mathrm{e^-}$$

$$\frac{1}{2}\,\mathrm{O_2} + 2\,\mathrm{H^+} + 2\,\mathrm{e^-} \longrightarrow \mathrm{H_2O} \tag{1.1}$$

The PEMFC has also some drawbacks; for instance it is not economically competitive compared to heat engines or other energy storage devices. This is due to the major cost of platinum loading catalyst [11], the low tolerance to fuel impurities and catalyst poisoning, as well as the water management that is not simple but necessary to maintain the PEM hydrated. These limitations can be overcome by increasing the PEMFC operational temperature from 80°C to well above 120 °C. By operating at these intermediate temperatures several benefits can play a role, such as higher tolerance to impure fuel and catalyst poisoning, alternative catalyst can be used for substituting common catalyst, and faster kinetics at the electrodes [13, 14]. The core of a PEMFC is the proton exchange membrane, in which typically needs water for the conduction of protons. Operating temperatures above 80 °C result in dehydration which consequently decreases the proton conductivity. Thus, a new generation of electrolytes is needed with high thermal stability and conductivity that hold at high temperatures and anhydrous conditions.

1.1.2 Electrolyte materials

Currently, polymer and aqueous electrolytes (water based ionic solutions) are known as the common electrolyte. This section discusses the electrolyte materials intended for use in a PEMFC. In general the requirements for a fuel cell electrolyte are [10]:

1. High ionic conductivity
2. Low electronic conductivity
3. Impermeability to fuel gases
4. High thermal stability
5. Ease of manufacturability

To date the best known and common electrolyte material used in PEMFC is based on perfluorosulfonic acid (PFSA). The most commonly used PFSA is produced by Dupont and is known as Nafion®, which in hydrated conditions has conductivity of 0.13 $\mathrm{S{\cdot}cm^{-1}}$ (at 70 °C) and a durability of 60,000 hours [12]. Nafion consists of a perfluoroethylene hydrophobic backbone that provides stable support and sulfonic acid hydrophilic side chains that promote the formation of

water clusters [15–17]. Significant development has been made on other types of perfluorinated based membranes to improve their ionic conductivity [18]. Ionic conduction is achieved by keeping the Nafion® in wet conditions, allowing the proton to transfer along the hydrophilic domain defined by the hydrated sulfonic acid groups. Proton transport in hydrated Nafion® involves two mechanisms; *i.e.* by proton hopping (Grotthuss) and proton diffusion along with the host molecule (vehicular) [12, 19].

Ionic liquids, more specifically protic ionic liquids, are suitable as anhydrous electrolytes for PEMFC. Portic ionic liquids display high thermal stability and consist only of ions, which is theoretically ideal for ionic conduction. Despite these benefits, protic ionic liquids displays relatively low conductivity because of their relatively high viscosity. For these reasons, I have undertaken a comprehensive study of protic ionic liquids properties, using different approaches that include modifying the protic ionic liquid's structure and mixing with another compound. These strategies are intended to have a significant impact in protic ionic liquids based electrolyte PEMFC.

1.2 Objectives of this work

As stated in the previous section, protic ionic liquids are suitable candidates as proton carrier for use in intermediate temperature PEMFCs. The distinct characteristic such as high thermal stability and high conductivity is the traits of these compound. The aim of this thesis, has been to prompt high proton conductivity in bulk protic ionic liquids, which I have addressed by mixing protic ionic liquid with other compounds and protic ionic liquid structural modification. My work has been limited to imidazolium based protic ionic liquids only.

In order to induce proton transfer, the ability to form an extended hydrogen bonded network is a prerequisite, compounds like water and imidazole are example that fulfil this requirement [20, 21]. Ethylene glycol (EG) shows the same tendency to form hydrogen bonds trough the hydroxyl groups, and has in some cases been studied mixed with aprotic ionic liquids. However ethylene glycol-protic ionic liquid mixtures had not been explored, therefore we focused on ethylene glycol-protic ionic liquid mixtures in wide composition range and their related properties for PEMFC such as ionic conductivity, fluidity and thermal behavior are investigated. Previous study on alkyl ammonium based protic ionic liquids using *ab initio* simulations showed that hydrogen bonds become stronger and more stable for higher alkyl chain lengths [22]. Hence in our second approach, protic ionic liquids are modified by attaching alkyl chains of different length on the cation to form stronger hydrogen bonds and hypothetically induce faster proton transport. Our investigation has focused on understanding the interactions established between cations and anions, the adopted nano-structuration, as well as the nature of charge transport.

1.3 Organization of this thesis

This thesis describes my work devoted to the characterisation of protic ionic liquids as proton conducting materials with the aim to address some challenges related to the fuel cell technology. Having pointed out the scientific context in **Chapter 1**, the organisation of this thesis is as follows. **Chapter 2** gives the background for ionic liquids such as history, synthesis and physicochemical properties. **Chapter 3** presents the experimental methods used to characterise the protic ionic liquids in this study. **Chapter 4** presents the main finding in the appended papers, **paper I** ethylimidazolium triflate is mixed with the co-solvent ethylene glycol, while **paper II**, focuses on modifying the imidazolium cation in alkyl-imidazolium bis(trifluoromethylsulfonyl)imide by varying the length of alkyl chain attached on the nitrogen atom. **Chapter 5** concludes this thesis with some focus on the future works that remain to be done.

2 Ionic liquids

Common industrial solvents are usually volatile organic compounds (VOCs), which are unfortunately also a major source of air pollution. There are a number of options for reducing this, such as using no solvents or using water, supercritical fluids, and ionic liquids instead. By virtue of having a low vapor pressure, the use of ionic liquids can contribute to reduce the environmental impact. In addition, their properties are tunable by changing the cation-anion pair, in fact they are also known as "designer solvents". Research activities on ionic liquids have been very intense the last decades, yet properties of ionic liquid blends and their applications in practical devices remain areas to investigate. This chapter gives a glimpse of ionic liquids with focus on their history, synthesis, and basic properties.

2.1 History

How the history of ionic liquids is described depends on the authors who report and on what definition is used. Ionic liquids are also known as low temperature molten salts, ionic fluids, or organic low melting liquids. The journey of the compounds that we today call ionic liquids dates back to the 19^{th} century, and is closely related to the field of molten salts [23–25].

The first low melting salt was made in 1914 by Paul Walden, for which he is now considered the founder of the ionic liquids field. The synthesised ionic liquid was EAN, ethyl ammonium nitrate, obtained from the neutralisation reaction of amine and nitric acid. His works became important also for determining the ionicity of ionic liquids based on the relation between fluidity and conductivity. EAN is the most widely studied ionic liquid up to today, but ionic liquids in general did not prompt significant interest until the late 80s, when Wilkes and Zoworotko worked on water stable ionic liquids. They introduced the imidazolium cation, in *e.g.* the ionic liquid 1-alkyl-3-methylimidazolium chloride alumunium chloride ($[C_nC_1im][Cl\text{-}AlCl_3]$ which stayed in the liquid state at ambient temperature. Undoubtedly, these findings drew the attention of scientists, as demonstrated by the increasing number of scientific articles published on the topic of ionic liquids, reflecting a new rapidly expanding field [23, 26, 27].

2.2 Classes of ionic liquids

Ionic liquids are composed of a cation and an anion, and the possible number of ionic liquids is predicted to be as high as 10^{16}, based on the known potential cation-anion pairs. There are several types of ionic liquids, such as Good's buffers ionic liquids, task specific ionic liquids, and acidic ionic liquids, but the most common classification distinguishes between protic ionic liquids (PILs) and aprotic ionic liquids (AILs). Both protic ionic liquids and aprotic ionic liquids display low vapor pressure and high ionic conductivity, and are therefore interesting as a new generation of electrolyes for use in energy conversion devices, offering safety in addition to performance [28–30].

Aprotic ionic liquids are extremely interesting for applications in lubrification, as solvent, in catalysis, or to dissolve cellulose. They have high thermal stability, and can form hydrogen bonds, which in the case of imidazolium cations, for example in $[C_4C_1im][Cl]$, and $[C_1C_1Im][TFSA]$ [31, 32], mainly involve hydrogen atoms sitting on the imidazolium ring. The high cohesive energy typical of aprotic ionic liquids makes viscosity high and hence also limits the ionic mobility. Protic ionic liquids are obtained by simple acid-base neutralisation reaction, which is a quite simple and cheap method, and compared to their aprotic ionic liquids counterparts display cation-anion interactions of a different nature.

2.3 Protic ionic liquids

The main content of this subsection is the protic ionic liquids' distinct feature that make them different from their aprotic analogue, the exchangeable proton. Protic cations have a H-atom typically bound to a nitrogen or phosphor atom, which is available for hydrogen bonding. Another interesting property of protic ionic liquids is their acidity, which is important in organic synthesis. There is strong correlation between acidity and reactivity, for example in the Friedel-Crafts alkylation of phenol with tert-butyl alcohol, the main products depend on the acidity of the catalyst. One of the methods used for evaluating the acidity in protic ionic liquids is ^{1}H NMR, which is sensitive to the chemical shift of the NH resonance [6].

As previously mentioned, protic ionic liquids are considered in this thesis as potential electrolytes for use in next generation PEMFC, therefore protic ionic liquids with a high conductivity are desired. Protic ionic liquids can be obtained trough proton transfer from Brønsted acid to Brønsted base, but the proton transfer process is highly influenced by acid strength index or ΔpKa of acid and bases involved in the reaction. Ideally, protons are completely transferred to the base, and in order to be classified as protic ionic liquids the purity should be higher than 99% [33]. However, in reality some of the protons are not fully transferred, which implies the presence of neutral acidic and basic species. This phenomena

cause worst performance in ionic conductivity, and motivate the development of approaches to evaluate the ideality of ionic liquids.

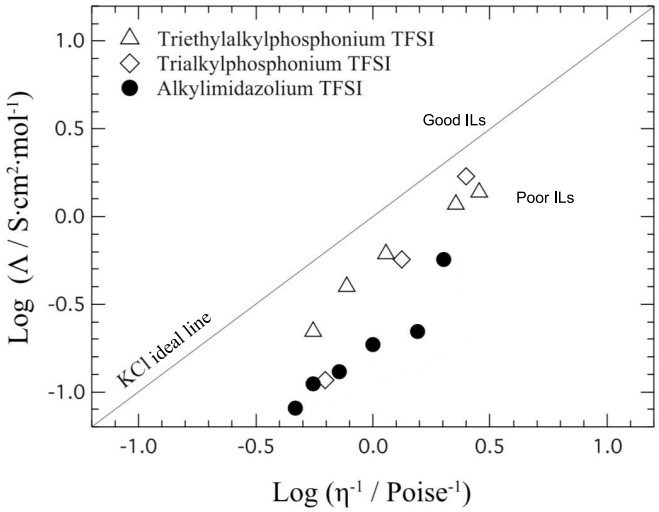

Figure 2.1: Walden plot for ionic liquids with various cations showing a behavior below the KCl ideal line

A concept used to measure qualitatively whether the compound is a good or a poor ionic liquid, is called "ionicity". The Walden plot, *i.e.* a plot of log fluidity versus log molar conductivity, has been widely used to assess the ionicity of ionic liquids, Fig 2.1. The ideal line is obtained from a diluted KCl solution, a system known for full dissociation and displaying ideal mobility [34]. Thus a suitable protic ionic liquid for next generation PEMFC, is one that has highly mobile ions and a close to ideal behavior on a Walden plot.

2.4 Synthesis

The archetypical protic ionic liquid, ethylammonium nitrate or EAN, is obtained by the neutralisation reaction between ethyl ammonium and nitric acid [23]; other protic ionic liquids can be synthesized in the same manner. Another method to synthesize ionic liquids is by the metathesis reaction, commonly used to obtain aprotic ionic liquids. In order to tune different properties, such as melting point, viscosity and liquidous range, the low symmetry of cations are needed and the anion is usually coming from a weak inorganic/organic base. The majority of cations used in ionic liquids synthesis are derived from a five membered heterocyclic ring such as imidazole, pyrazole, and triazole, while anions can be halides, nitrates, sulfates, alkylsulfates, alkylsulfonates, $[BF_4]^-$, $[PF_6]^-$, $[CH_3CO_2]^-$, $[CF_3CO_2]^-$, $[Tf_2N]^-$.

Among all available anions, fluorinated anions are commonly selected since they result in lower viscosities as a consequence of less van der Waals interactions [6, 35].

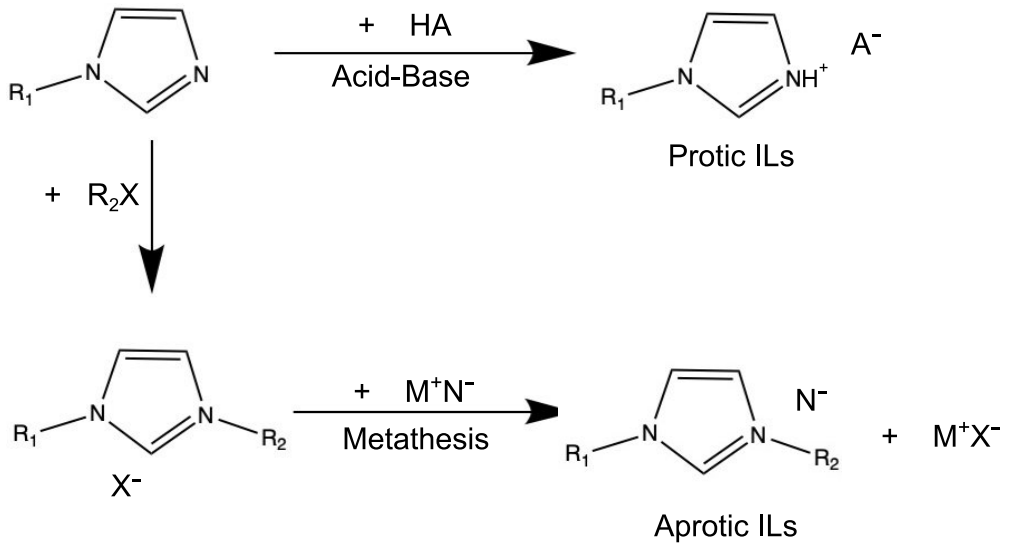

Figure 2.2: Synthesis routes used to obtain protic and aprotic ionic liquids

Aprotic ionic liquids are commonly synthesised by metathesis reaction from halide or similar salt of a desired cation while protic ionic liquids are formed by proton transfer from Brønsted acid to a Brønsted base at equimolar composition, Fig 2.2. Angell and Yoshizawa stated in their work that the degree of proton transfer from Brønsted acid to Brønsted base is a function of ΔpKa, the stronger acid or base the greater driving force for the reaction to occur. They also proposed that $\Delta\text{pKa} > 10$ is required to obtain full proton transfer [6, 34].

2.5 Properties of ionic liquids

This section gives a brief background about the properties of protic ionic liquids and describes the factors that govern them. The elucidation of factors that govern the transport properties of protic ionic liquids play a key role in designing protic ionic liquids and its performance as electrolyte material in next generation PEMFC. The cation or anion size, molecular interaction, and the magnitude of interaction will affect not only the thermal stability but also the transport properties such as viscosity, ionic conductivity, and self diffusion coefficient of the ionic species.

2.5.1 Thermal stability

Thermal stability is very important in high temperature applications for ionic liquids *e.g.* solvents for organic reactions at high temperature, solvents for cellulose, thermal energy storage (TES) and heat-transfer fluids (HTFs), high-temperature lubricants, and high recovery in manufacture [36], moreover high thermal stability could help the advancement of next generation PEMFC. However, there are also ionic liquids that are not very stable, which easily decompose and evaporate. This can produce impurities and cause environmental problems as VOCs do. Among available techniques, Thermogravimetric analysis (TGA) is the most used to determine the thermal stability of ionic liquids, commonly through a single linear heating scan over a wide temperature interval. The thermal stability of ionic liquids is usually characterised by significant mass losses at high temperature decomposition (T_d or T_{onset}), which can be obtained from the intersection of the baseline weight and the tangent of the weight dependence on the temperature curve as decomposition occurs.

Mass losses in ionic liquids are caused by two phenomena; decomposition or evaporation. Decomposition of ionic liquids refers to the degradation of substances which is induced by a chemical reaction. While evaporation is a physical process from the liquid to the gaseous state without the formation of new substances. The molecular structure of cations and anions plays an important role in ionic liquids thermal stability. For example, by keeping the alkyl-substituted carbons identical, the volatility of ionic liquids with an asymmetric cation is lower than that with a symmetric cation [37].

2.5.2 Molecular interactions

Molecular interactions in ionic liquids are complex, and depend on the charge as well as on the molecular and electronic structure of the constituting ions. Thus the elucidation of ILs' molecular interactions are challenging yet fruitful to understand in designing ionic liquids for specific purposes. Coloumbic interaction, hydrogen bonding, and dispersion forces are dominating in ionic liquids. In principle these interactions can be studied by number of experimental techniques such as infrared, Raman, ^{1}H NMR or other related analytical methods [31, 38–40].

Among the forces present in ionic liquids, Hydrogen bonding plays key role in ionic liquids development for application purposes, it is one of the controlling factor that has significant impact on the ability of ionic liquids to dissolve compounds otherwise not soluble in other solvents or act as proton conducting media [40].

Among all available ionic liquids, imidazolium cations are the most investigated, the hydrogen bonding that exist in either aprotic ionic liquids or protic ionic liquids are believed as one of the main attracting point, even though the strength and nature of hydrogen bonds is still vividly debated. The key property that dis-

tinguish protic ionic liquids from other aprotic ionic liquids is the proton transfer from the acid to the base, resulting in the formation of proton donor and proton acceptor sites, which can be used to build up a hydrogen-bonded network. In the case of aprotic ionic liquids the hydrogen bonding is weakly formed between the hydrogen atoms in hetero alkylic groups on cations and electronegative atoms on anions. Meanwhile in protic ionic liquids the hydrogen bond is a strong interaction between the -NH site on the cation and the anion [32]. Protic cations tend to have a H-atom attached directly to a charge carrying nitrogen or phosphor atom, and based on the general measure with respect to "donor strength", the order of hydrogen bond strength can written as O-H > N-H > S-H > C-H. To conclude, protic ionic liquids are expected to form stronger and more directional hydrogen bond than aprotic ionic liquids [31]. Direct experimental techniques and simulations are established to demonstrate the existence of hydrogen bond interaction in ionic liquids.

2.5.3 Nanostructure

Bulk ionic liquids were initially thought of as common solvents, *i.e.* as homogenous molecular systems. However, recent experiments and computational results suggest that ionic liquids can form heterogenous structures at nanoscale level [41]. The degree of nanostructuration in ionic liquids depends on several aspects; coloumbic interaction, packing geometry, cation-anion structure and hydrogen bonding [41]. For example, the nanostructure in ionic liquids becomes more obvious as the alkyl chain on the cation or anion increases, this is because the segregation of charged and uncharged species are more pronounced. Different anion types also influence ionic liquids nanostructure, as recently shown when comparing $[P_{6,6,6,14}][Cl]$ with $[P_{6,6,6,14}][Tf_2N]$, where the $[Cl]^-$ anion leads to more defined nanostructures than the $[Tf_2N]^-$ anion [42].

A variety of experimental techniques are employed to describe ionic liquid bulk structure that segregates into non-polar and polar domains using, *e.g.* small angle neutron scattering (SANS) and small angle X-ray scattering (SAXS) [42]. Russina and co-workers demonstrated and explained the heterogeneity in 1-alkyl-3-methylimidazolium bis(trifluoromethane)sulfonylamide ($[C_nmim][NTf_2]$), n from 1 to 10, by the use of small-wide angle X-ray scattering (SWAXS). They used Bragg's law, $d = 2\pi/q_{max}$ to describes three distinct peaks, where d is the correlation length and q_{max} is the peak position at maximum intensity. The strong intensity in low q region is highly dependent on the length of the alkyl chain, a signature of structural heterogeneity [43].

2.5.4 Transport properties

Fluidity

The high conductivity of liquid electrolytes is generally associated to a low viscosity. Viscosity describes the internal resistance of a fluid to flow, and has the units of poise or Pa·s. The viscosity in ionic liquids depends on intrinsic factor e.g. the ions size, ion-ion interactions (coulombic interaction, van der Waals force and hydrogen bonds), and extrinsic factor e.g. temperature and pressure. For example, delocalisation of the charge on anion, such as through fluorination, decreases the viscosity by weakening hydrogen bonding. Consequently, fluorinated anions are preferable to be used in ionic liquids synthesis. Another aspect that govern the viscosity in ionic liquids is the cation structure, previous investigation by Greaves et al. on 25 ionic liquids showed that increasing the length of alkyl chains increases the viscosity through stronger Van der Waals interactions. Interestingly, they also noted that the substitution of functional group by alkyl chain gives significant effect on the viscosity is attributed to stronger hydrogen bonding, ion-ion interactions and asymmetry of the molecules [44].

Diffusion

Diffusion, a phenomenon of particles motion, depend on several factors such as pressure, temperature, and concentration. In a system where the diffusion occurs in x-direction related to concentration gradient, it can be written as follow :

$$\bar{J} = -D\frac{dC}{dx} \tag{2.1}$$

where J is molecular flux, D is self-diffusion coefficient, and C is concentration. D represent rate of motion in certain area over a unit time or m^2/s. In classical hydrodynamic, the Stokes-Einstein equation relates D of a particle (or a molecular species) to its effective hydrodynamic radius r_s, the viscosity of the medium η, temperature, and c is the shape factor (4 to 6) (eq. 2.2) [45].

$$D = \frac{k_B T}{c\pi\eta r_s} \tag{2.2}$$

Compared to the gaseous state, in liquids molecules are more densely packed and display smaller self-diffusion coefficients. In thermodynamically equilibrium condition, the individual molecules in liquid move with random translational motion. The motion is characterised as random walk of the particle, or called Brownian motion. Diffusion NMR is employed in this work to study the ionic transport of protic ionic liquids with focus on the proton's motion. The occurrence of a Grotthuss, or hoping, mechanism is indicated by protons diffusing faster than the parent molecule.

Conductivity

In general, conductivity relies on a variety of aspects: the concentration of charge carriers (C), the charge they carry (Z) and their mobility (μ). According to this definition, conductivity, σ, can be written as :

$$\sigma = (|Z|F)C\mu \tag{2.3}$$

the absolute symbol is to ensures that conductivity value is always a positive number and F is Faraday constant. Ionic conductivity unit is Siemens·cm^{-1}.

Ionic liquids have been proposed as new electrolyte materials in new generation PEMFC due to several striking features such as high concentration of ions and high mobility of the ions, which theoretically make them excellent as electrolytes. However in reality, ionic liquids conductivity is limited due to a certain aspects such as the diffusivity, viscosity, and ion sizes. Moreover, in protic ionic liquids the conductivities are low due to the fact that the ion-pairs and neutral species are present thus limiting the concentration of ionic species. According to Yaghini et al., the conductivity of aprotic ionic liquids is higher than their analogous protic ionic liquids, which arise from higher viscosity of protic ionic liquids.

Proton transport mechanisms

There are two types of proton transfer mechanisms; vehicular and Grotthuss (proton hopping) mechanism, Fig 2.3. In the vehicular mechanism, the proton is transported by the host molecule through a translational movement, in this case the protonic migration is highly dependent on diffusion process. In the Grotthuss mechanism, the proton is decoupled from the host molecule and moves through structural diffusion of the hydrogen bonds [46]. The formation and breaking hydrogen bonds is a requisite for this process to occur.

In ionic liquids the proton transport could be due to several mechanisms: vehicular, Grotthuss or a combination of these two. Appropriate analytical methods are necessary to verify the occurrence of the Grotthuss mechanism. NMR spectroscopy is used to determine proton conduction mechanisms, more specifically pulsed-field gradient (PFG)-NMR was implemented to measure differences in the diffusivity coefficient of available species (proton and cation). One way of examining the occurrence of Grotthuss mechanism is through the ratio of protonic diffusion over cation diffusion, if its above unity than it can be conclude that there is occurrence of Grotthuss mechanism [39, 47]. To conclude, the proton transfer mechanism are one of the key component in improving the ionic liquids performance, in term or protonic conduction. Hence varying approaches are required to induce this phenomena, one is to add second compound with the proton donor ability to build hydrogen bond network in the system another is to modify the cation structure that make the hydrogen bond stronger and promote the proton decoupled motion.

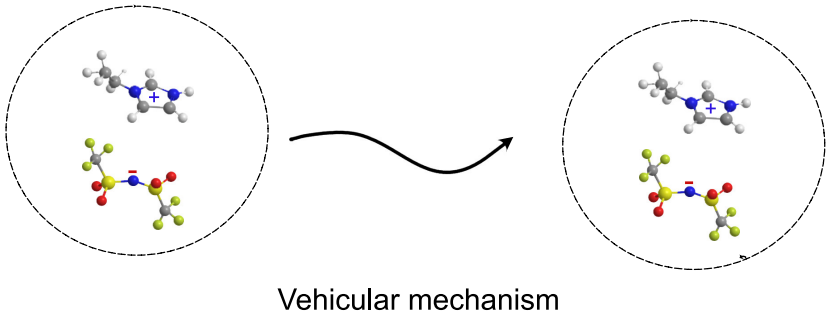

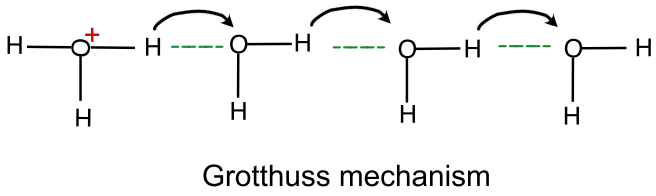

Figure 2.3: Illustration of various proton transport mechanisms, vehicular mechanism in $[C_2HIm][TFSI]$ and Grotthuss mechanism in water

3 Experimental methods and procedures

3.1 Thermal analyses

How materials change their properties with temperature, for example during heating or cooling treatment, is a basic yet important information. In this thesis thermal analysis was applied to investigate the thermal stability and phase behavior of protic ionic liquids (PILs), whose intended application is in intermediate temperature PEMFCs. More precisely, thermogravimetric analysis and differential scanning calorimetry have been used.

3.1.1 Thermogravimetric analysis (TGA)

Thermogravimetric analysis (TGA) is widely used to study the thermal stability of materials through their mass changes as a function of temperature or time. TGA can give information about decomposition kinetics, lifetime or thermal stability, multicomposition system and oxidative stability of materials. The material can loose or even gain mass during the heating processes due to several phenomena:

1. Evaporation of volatile compound
2. Oxidation of organic material in contact with air or pure oxygen
3. Thermal decomposition
4. Water uptake (if humid purge gas is used)

TGA uses a high sensitivity balance in a controlled temperature and gas atmosphere. A number of factors should be considered when performing TGA experiments, such as sample preparation, heating rate (there are two options, heating by constant heating rate or called dynamic, and heating at constant temperature or isothermal), types of crucibles and the nature of the purge gas. Various purge gases can be used for studying the degradation or decomposition behaviour of materials in different atmospheres [48].

In this work, the analysis of protic ionic liquids was carried out using a TGA/DSC 3+ from Mettler Toledo equipped with an autosampler, covering temperature ranges from 25 °C up to 1200 °C. In this work, the temperature was typically set from 25 °C to 400 °C, a suitable range to extend the thermal stability that for

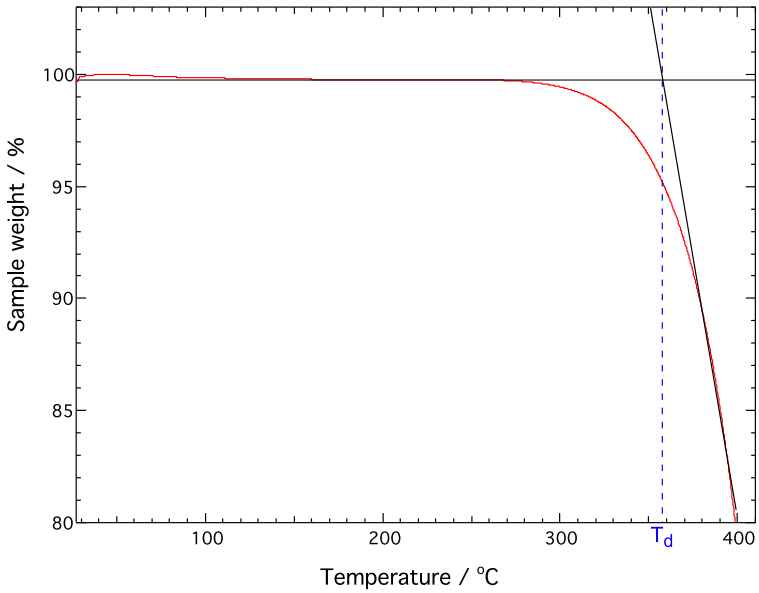

Figure 3.1: The typical plot of thermogravimetric analysis result, here for the sample $[C_2HIm][TFSI]$

investigated protic ionic liquids is expected to be above 100 °C to fit the PEMFC requirements. The samples (typically 3-20 mg) were placed in open aluminum 100 µl crucibles, and were heated at 10 °C·min^{-1} under nitrogen flow for paper I, and under air flow at rate 20 mL·min^{-1} in paper II. A typical plot obtained from a TGA experiment is given in Fig. 3.1.

3.1.2 Differential scanning calorimetry (DSC)

DSC is a complementary and valuable method to material scientists. It is easy to operate, requires little sample preparation, and provides a wealth of useful information. DSC is sensitive to heat flow changes between a sample and a reference as a function of time and temperature, during heating or cooling processes. Qualitative and quantitative results on physical or chemical properties can be detected by [49]:

1. Melting and enthalpy of fusion
2. Crystallisation and supercooling
3. Solid-solid and solid-liquid transitions
4. Glass transitions

There are two different types of DSC, *i.e.* 1) power compensated and 2) heat flux DSC; the latter is the one used in this thesis. Inside a heat flux DSC cell there are two platforms for sample and reference crucible (typically empty). The crucibles are placed over the DSC sensors. The sensors are usually connected through a

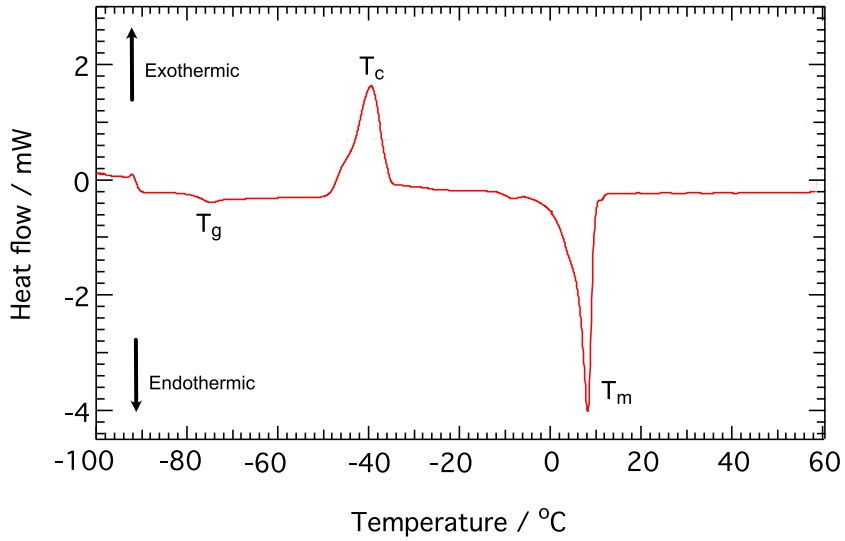

Figure 3.2: Example of typical DSC curve of a protic ionic liquid. The sample was cooled fast and followed by subsequent heating at a rate of 5 K·min^{-1}.

thin disc ceramic to the metallic part of the furnace. As the temperature of the furnace is increased, the heat flows to the disc and the crucibles. The heat flows radially trough the thermal resistance of the sensors, the temperature difference across this thermal resistance is measured by the radially arranged thermocouples expressed as:

$$q = \frac{\Delta T}{R} \tag{3.1}$$

where q is the heat flow, ΔT is the temperature difference between sample and reference, and R is the thermal resistance from the sensor disc. The resulting typical DSC plot is shown in Fig. 3.2. In principle, DSC measures the heat flow in or out of a sample. By convention, the heat flow is exothermic or endothermic. Exothermic occurs when heat is released for example when a material crystallised and endothermic occurs when the material absorb heat and change the phase behavior from solid to liquid, Fig. 3.2. DSC is also able to measure the heat capacity changes of a material or glass transition temperature (T_g), which typically seen as a step baseline in DSC thermogram. T_g is temperature at which a glass forming material changes its state from liquid to disordered and rigid [48, 49].

All the calorimetric measurements were performed with a DSC2 instrument from Mettler Toledo equipped with a Huber TC-125MT Intracooler cooling system. This system can work from -100 to +500 °C at heating rates 0.02 to 300 K·min^{-1} or cooling rates at 50 °C·min^{-1}. The samples were always placed in hermetically sealed aluminum crucibles, the sample size ranging from 3 to 7 mg.

Nitrogen was used as the purging gas in this process. For paper I, the experiment covering temperature span from -120 to +130 °C, the protic ionic liquid-ethylene glycol samples were first quickly cooled from 25 °C to -120 °C at a cooling rate of 20 °C·min^{-1}, then followed by subsequent heating scan at a rate of 10 °C·min^{-1} up to 130 °C. In paper II, the cooling and heating rate were set to 10 and 5 °C·min^{-1}, and the covered temperature window spanned from -100 to +60 °C.

3.2 Vibrational spectroscopy

Vibrational spectroscopy is here used to investigate the local coordination in the protic ionic liquids. Both Raman and infrared spectroscopy were used in this work, which are complementary techniques. Raman is more sensitive to symmetric vibration of non polar molecules, while asymmetric vibrations of polar molecules are better seen by infrared. Vibrational spectroscopy can be used for a wide variety of samples and can provide information both qualitatively and quantitatively. Vibrational spectroscopy offers several advantages, such as ease of sample preparation, it is generally non invasive, and small amount of sample is needed. In the context of my thesis, vibrational spectroscopy is used to study the nature of cation and anion interactions, molecular conformation and hydrogen bonding in pure or mixed protic ionic liquids.

The basic principle of vibrational spectroscopy can be described by the classical harmonic oscillation theory of two bonded atoms, considered as two vibrating masses (m_1 and m_2) connected by a spring (representing the chemical bond), according to equation 3.2:

$$\bar{v} = \frac{1}{2\pi c}\sqrt{\frac{k}{\mu}} \tag{3.2}$$

where $\bar{v}$ is the vibrational frequency of the atoms in inverse centimeters (cm^{-1}), k is the force constant of the bond, c is the velocity of light and μ is the reduced mass of the system, i.e.

$$\mu = \frac{m_1 m_2}{m_1 + m_2} \tag{3.3}$$

As shown in equation 3.2, a higher force constant or a stronger bond, results in a higher vibrational frequency. Heavier atoms (higher value of μ) result in lower frequencies.

3.2.1 Infrared spectroscopy

In infrared the sample is irradiated with a light source of intensity I_0. I_0 will be absorbed by the molecules at specific frequencies, and the transmitted radiation,

I_s, is typically of lower intensity. The energy radiation transmitted by the sample, I_s, is collected by a detector and presented in intensity versus frequency plots either in the absorbance or transmittance mode. Fig. 3.3 illustrates the working principles of infrared spectroscopy.

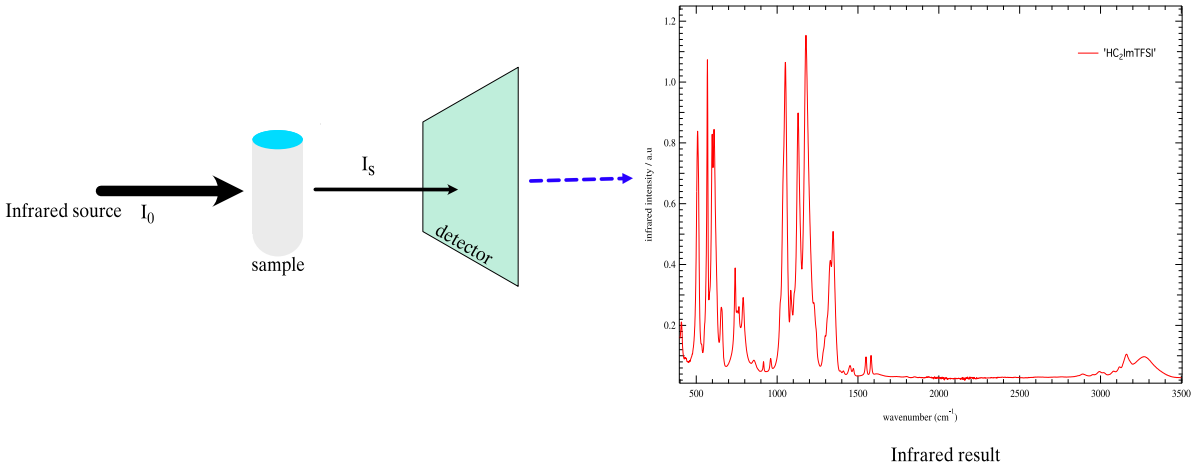

Figure 3.3: Infrared spectroscopy sketch and typical graph result

Molecular vibrations are associated to changes in bond lengths and bond angles, and can be classified as wagging, stretching, scissoring, rocking, bending and twisting. Infrared spectrometers can be used in several reflection modes, such as specular reflectance, diffuse reflectance, and attenuated total reflectance (ATR). The latter has been used in this thesis work. The infrared spectrum is typically divided into three regions: *far-infrared* <400 cm^{-1}, *mid-infrared* 400-4000 cm^{-1}, and *near-infrared* 4000-13000 cm^{-1}.

To collect infrared spectra of protic ionic liquids and protic ionic liquid mixtures, a Perkin Elmer spectrometer was used, which is equipped with an ATR crystal and is most suitable for investigating liquid and gel-like samples. Droplets of the liquid were poured over a single reflection diamond crystal, accumulating 32 scans and covering the spectral range 400-4000 cm^{-1}. The spectral resolution was 2 cm^{-1} and all measurements were performed in open air and at room temperature.

3.2.2 Raman spectroscopy

In Raman spectroscopy, the measurement is based on a scattering process during which light and matter interact. The material is irradiated with intense monochromator light source resulting scattered light with different intensity and vibration frequency. Lasers are chosen as excitation source due to the beam are highly monochromatic, laser beam diameter is relatively small (it can be reduced to a smaller diameter by a simple lens system). Raman has two types of scattering, Reyleigh and Raman scattering. Reyleigh scattering occurs when the scattered

light has the same energy (hence frequency) as the incident light, whilst Raman scattering appear in lower or higher frequency, $v_0 \pm v$, and is also distinguished into Stokes and anti-Stokes scattering, see Fig. 3.4

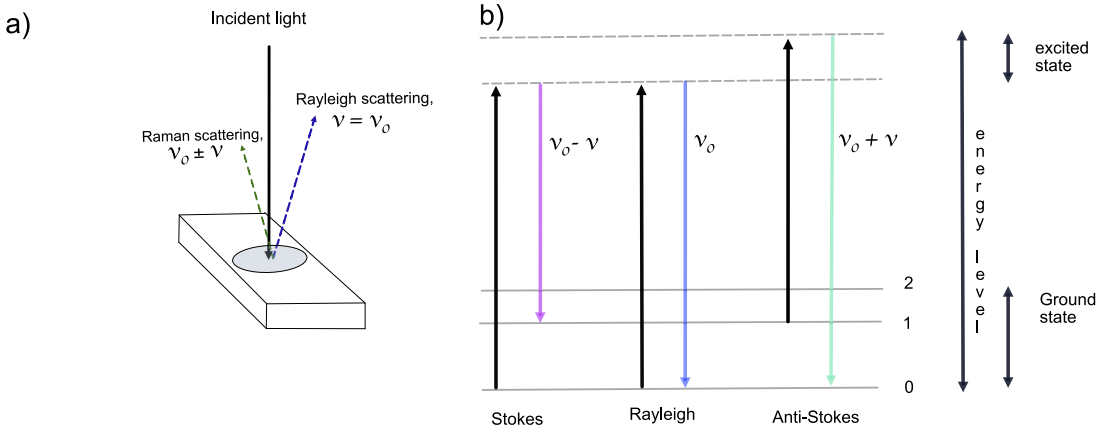

Figure 3.4: General schematic for a) Raman spectroscopy and b) Scattering types : Stokes, Rayleigh, Anti-Stokes

In this work, Raman spectra were recorded with InVia Raman spectrometer from Renishaw® equipped with four lasers, 514, 532, 633, and 785 nm. Laser with λ 785 nm was used as the excitation source for collecting the spectra of protic ionic liquids series in this thesis. The instrument also equipped with three different grating, 1200, 1800 and 2400 l/mm. In paper I and paper II the measurement was performed using 785 nm lasers equipped with 1200 l/mm grating, the laser power was set to 3 mW at the sample, the spectrometer was calibrated with Si wafer at 520.6 cm^{-1} with spectral resolution 2 cm^{-1}. The sample was prepared inside NMR tubes and measured at room temperature. Typically, spectra collected in the spectral range from 80-4000 cm^{-1} and accumulation 10-20 scans with 10 second exposure time.

3.3 X-ray scattering

X-ray Scattering is based on the analysis of scattered X-ray pattern; the scattering of incident X-ray is caused by differences in the average electron density. X-ray scattering usually used for study the structure, shape, size, and structural orientation of a compound. This method has the ability to measure any object with spatial variation in electronic density (contrast), it could be liquid or solid, amorphous, crystalline particle, voids (pores, blisters, cracks, or crazes). Fig. 3.5, shows working principle of X-ray scattering instrument.

If assumed the scattering process is elastic, the incident wave impinge the matter is equal energy to the wave scattered, $|k_0| = |k_1| = 2\pi/\lambda$, but having different

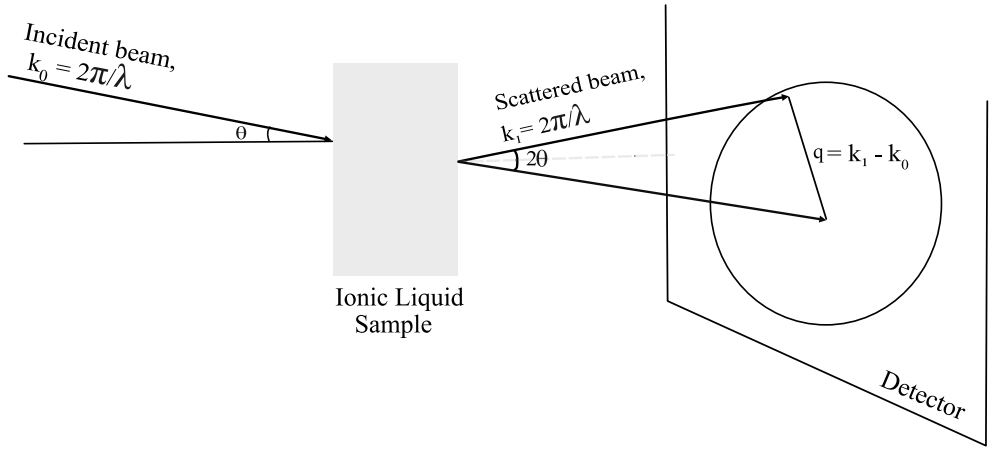

Figure 3.5: Schematic illustration on small angle X-ray scattering working principle

direction and 2θ is the scattering angle, Fig. 3.5. The wave vector (q) describes the position of the collected X-ray on the detector.

$$q = k_1 - k_0 \tag{3.4}$$

$$q = |q| = \frac{4\pi}{\lambda} sin\theta \tag{3.5}$$

The real spacing (d) can be calculated from a diffraction peak based on Bragg's law, where q is the position of the diffraction peak:

$$d = \frac{2\pi}{q} \tag{3.6}$$

In this study, Mat:Nordic SAXS/WAXS/GISAXS instrument at Chalmers Material Analysis Laboratory was used to collect data presented in paper II. This instrument can measure in three q-range regions: 0.07-2.7 $Å^{-1}$, 0.02-0.7 $Å^{-1}$, and 0.007-0.25 $Å^{-1}$. In order to obtain correct and reliable data, standard calibration is needed. Silver behenate (AgBeh) was chosen as reference to accurately determine the q range value. The accessible q range in this experiment are 0.07-2.2 $Å^{-1}$, and all measurement performed at ambient temperature.

3.4 Transport properties

3.4.1 Density

The density of a liquid is a basic yet important property that can have impact on heat, mass and momentum transfer. Density can be determined by various

methods: volumetric, isochoric, bouyancy, and vibrating bodies densitometer, the latter has been used in this work [50]. The density was measured using vibrating U-tube densimeter which can handle homogenous liquid, light slurry and gases. Liquid density was measured electronically using the frequency oscillation of the oscillator (U-tube). The density value was obtained from the correlation between oscillation period and the instrument constants [51], according to equation 3.7. The instrument provides sensitive, fast and precise measurement of density with uncertainty ± 0.00001 g·cm^{-3}.

$$\rho = A\tau^2 - B \tag{3.7}$$

Density ρ measurement was performed using an Anton Paar DMA 4500. The protic ionic liquids sample, approximately 1 ml, are loaded into the glass tube, and was measured using U-tube oscillation method. The density instrument can measure liquid density between 0 to 3 g·cm^{-3}, within temperature range of 0 to 100 °C with temperature uncertainty ±0.002 °C. The instrument was calibrated with water at 25 °C prior to any measurements.

3.4.2 Viscosity

Newton described the resistance to motion of fluid was attributed to "internal friction" which is called viscosity. He postulated that the force (F) per surface area (A) required to maintain the motion of a fluid between two plates is proportional to velocity gradient (u/h), and viscosity (η), as expressed in equation 3.8. For simplicity, this is often illustrated as a fluid sandwiched between two parallel plates as shown in Fig. 3.6 [52, 53].

$$\frac{F}{A} = \eta(\frac{u}{h}) \tag{3.8}$$

$$\tau_{xy} = \eta\dot{\gamma}_{xy} \tag{3.9}$$

Equation 3.8 can be written in terms of shear stress and shear rate which is shown as equation 3.9, where τ_{xy} is shear stress in x axis with normal direction pointing y ordinate, and $\dot{\gamma}_{xy}$ or shear rate deformation of the fluid. Commonly, liquid that follows Newton's postulate is called newtonian liquid, where its shear rate is proportional to its shear stress is known as Newtonian liquid, otherwise it is called non-Newtonian. There are various way to measure viscosity, such as capillary method, falling sphere method, plastometer method, and rotational rheometry method (parallel or cone and plate) [54].

The viscosity of the ionic liquids studies in both paper I and II were determined using cone and plate rotational rheometry. In paper I, the viscosity is measured by Antoon Paar MCR 300 with cone and plate geometry with a diameter 50 mm, an angle of 1°, and trunctuation gap 52 μm. Whilst in paper II, the DRH 3 from

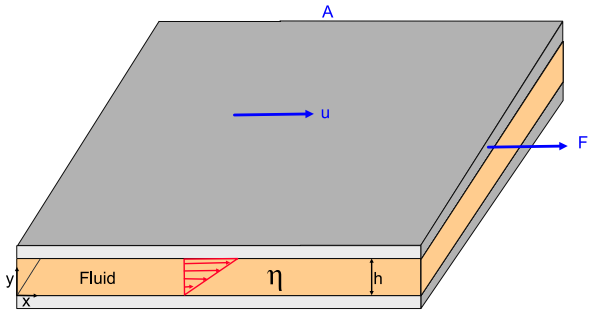

Figure 3.6: A simple representation of a fluid placed between two parallel plates in cartesian coordinate

TA instrument equipped with peltier plate was used, it has the ability to measure in wide range temperature from -40 to 200 °C and temperature accuracy ± 0.1 °C, cone and plate geometry with an angle of 1°, trunctuation gap 26 μm, and 40 mm of diameter were used. All measurements were conducted at room temperature.

3.4.3 Ionic conductivity

To study the ionic conductivity of protic ionic liquids, a broadband dielectric spectrometer can be used. Dielectric spectroscopy or known also as impedance spectroscopy was used in order to get the conductivity data. The principle of dielectric measurement is shown in Fig 3.7a, the sample material is placed between two electrodes that acts as sample capacitor. In an impedance measurement, however, sinusoidal alternating current voltage (U_0) with fix frequency $\omega/2\pi$ are applied to the sample causes a current I_0 at the same frequency in the sample.

In paper II, broadband dielectric spectroscopy from Novocontrol GmBh was used. The liquid was placed in between two identical gold-pated brass electrodes 13.5 mm in diameter, separated with 1 mm silica spacer for obtaining controlled liquid thickness, see Fig 3.7b. The conductivity measurements performed in frequency range 10^{-1} - 10^{7} Hz and temperature range varies from -60 to +250 °C, the temperature controlled using nitrogen cryostat with uncertainty ±0.5 °C, each temperature was set 600 second for stabilisation. Conductivity was measured at every 10 °C.

In case of ionic conductivity measurement of protic ionic liquid-ethylene glycol mixture, paper I, CDM 210 conductometry was employed, standard calibration solution was chosen for obtaining reliable result using aqueous KCl (0.01 M) before each measurements. The samples was equilibrated for 30 minutes at 30 °C with temperature uncertainty ±0.1 °C.

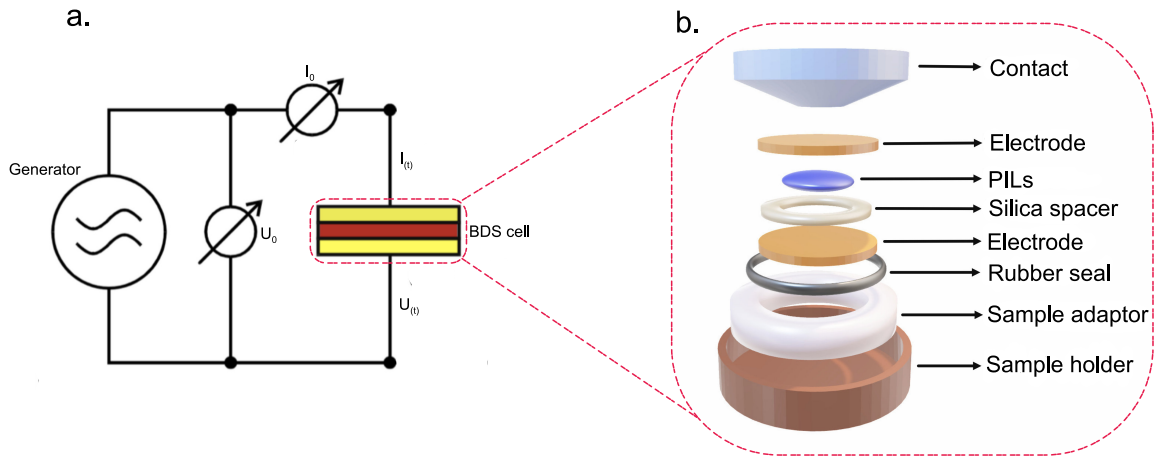

Figure 3.7: Schematic figure for: a) Broadband dielectric spectroscopy measurement, and b) The broadband dielectric spectroscopy cell used in this thesis

3.4.4 NMR spectroscopy

Nuclear magnetic resonance (NMR) spectroscopy is an analytical method which utilises the spin behavior of atomic nuclei. The common nuclei that posses spin are ^{1}H, ^{15}N, ^{13}C, and ^{19}F, and the nucleus of interest in this thesis is mainly proton. A nucleus is a charged particle, when it spin it generates a magnetic field. When an external magnetic field (B_0) is applied, the magnetic orientation of the nuclei can orient aligned or against the applied field, see Fig 3.8. In NMR, the spectrum intensity is plotted as a function of chemical shift. The chemical shift is commonly given in ppm, and different nuclei in a molecule give rise to different chemical shift.

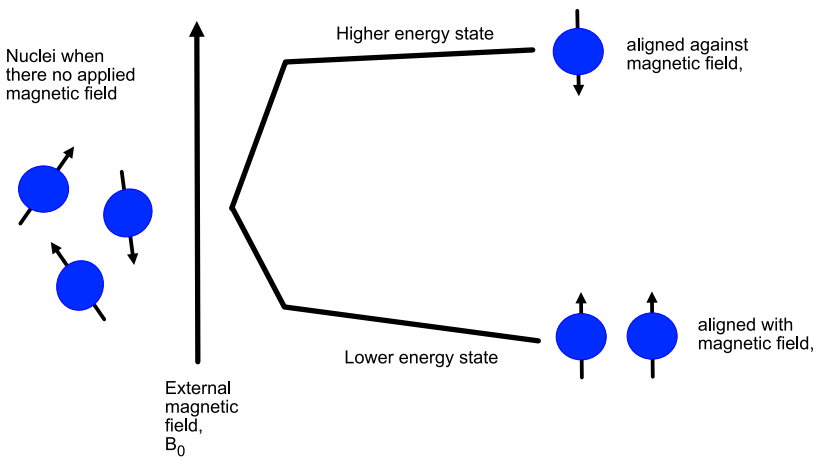

Figure 3.8: Spin states of proton in the presence of external magnetic field (B_0)

Diffusion NMR

Pulsed-field gradient NMR is useful for measuring diffusion in ionic liquids. The PFG NMR was first theoretically and experimentally demonstrated by Stejskal and Tanner and is still applicable for obtaining self-diffusion coefficient of ionic liquids [55]. A typical experiment to acquire self-diffusion coefficient consist a set of spectra employing to different values of the field gradient strength, G, or the length of the gradient pulse, δ, while the other parameters are held constant. Then, by plotting the normalised intensity (I/I_0) versus G or δ, the diffusion coefficient obtained by fitting the decay of the signal with the Stejskal-Tanner equation [55]:

$$I = I_0 \cdot exp^{-k} = I_0 \cdot exp - (\gamma \delta G)^2 D(\Delta - \delta/3) \tag{3.10}$$

where I is the signal intensity, I_0 is the signal intensity of spin-echo at zero gradient including T_1 and T_2 terms, D is the self-diffusion coefficient, γ is the gyromagnetic ratio, δ the length of the gradient pulse, and Δ is the diffusion time. Self-diffusion coefficient (D) can be extracted from the slope of the normalised intensity (natural logarithmic scale) versus k.

In this thesis pulsed field gradient nuclear magnetic resonance (PFG NMR) experiments were performed on a Bruker Avance 600 spectrometer. In paper I, the maximum gradient used for each sample was set in the range 200-400 $G \cdot cm^{-1}$. The pulse duration δ was set to 1 ms, and the diffusion time Δ 100 ms for all samples. In paper II, the applied linear gradient was varied in the range 0-550 $G \cdot cm^{-1}$, the pulse duration δ was set to 2 ms with the diffusion time Δ of 100 ms. The number of acquisitions in each experiment was 32 and relaxation delay of 15 s.

4 Results and discussion

The results discussed in this thesis are summarised from the two appended papers. The effect of adding ethylene glycol (paper I) or introducing structural modifications on imidazolium cations (paper II) to the thermal stability, ionic mobility and molecular interactions are discussed in this chapter. The main findings on the nanosegregation of protic ionic liquids are also reviewed.

4.1 Thermal stability

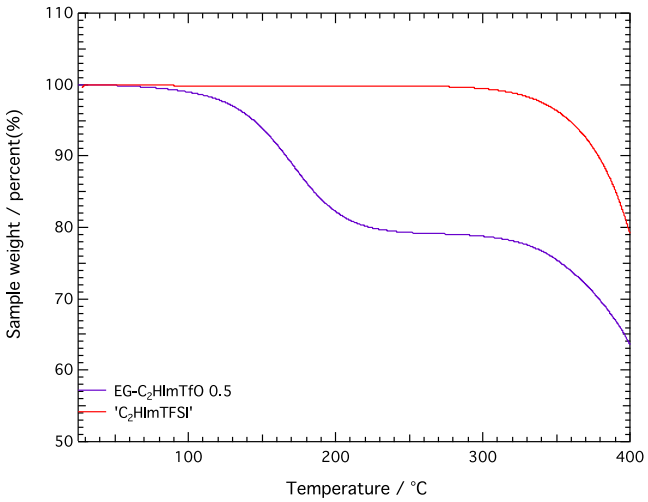

Figure 4.1: Thermal stability comparison for selected system, $[C_2HIm][TfO]$-ethylene glycol at 0.5 mole fraction of ethylene glycol and neat $[C_2HIm][TFSI]$

Figure 4.1 shows the thermal stability of protic ionic liquid-ethylene glycol mixture (0.5 mole fraction of ethylene glycol) and pure $HC_2ImTFSI$ during heating process from 25 °C to 400 °C with constant heating rate. These results indicate that the factor limiting the temperature window of operation of the protic ionic liquid-ethylene glycol mixture is the evaporation of ethylene glycol, not the chemical (in)stability of the protic ionic liquid itself.

A main finding from paper II is thus that even long chain protic ionic liquids are rather stable upon increased temperature, however the purity of the liquids and the extent of proton back transfer are crucial to control. The thermal stability obtained from TGA of all protic ionic liquids investigated in this work shows

decomposition temperatures above 100 °C. This is considered advantageous when considering protic ionic liquids as new electrolytes for next generation PEMFCs.

4.2 Intermolecular interactions

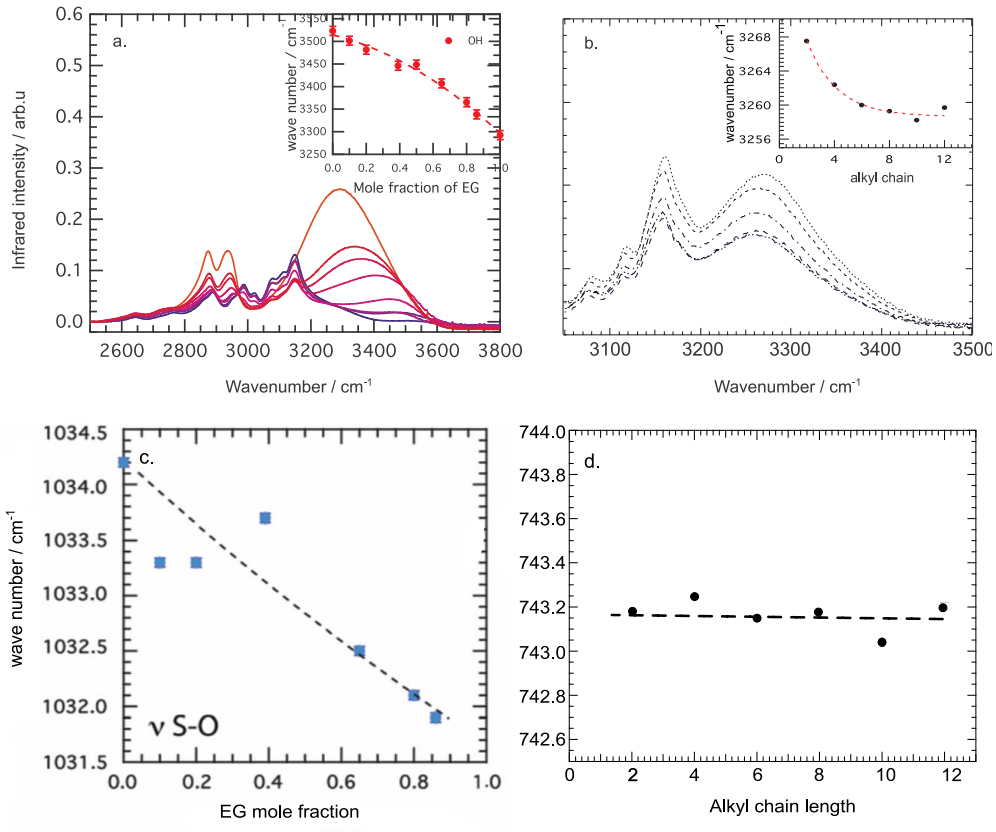

Figure 4.2: High frequency region of infrared spectra of a) [C_2HIm][TfO]-ethylene glycol mixtures, b) [C_nHIm][TFSI] series; and Raman wavenumber of c) S-O stretching mode for [C_2HIm][TfO]-ethylene glycol mixtures as a function of ethylene glycol mole fraction, d) Symmetric bending modes of CF_3 for [C_nHIm][TFSI] series as a function of n

In this work, the cation-anion interaction in protic ionic liquids and protic ionic liquid mixtures has been studied by infrared and Raman spectroscopy. Infrared spectroscopy is suitable to investigate the state of the cation, while Raman spectroscopy is a proper method to observe the state of the anion. The infrared and Raman spectra of [HC_nIm][TFSI] and [HC_2Im][TfO]-ethylene glycol mixture are shown in Figure 4.2. The infrared spectrum of [HC_2Im][TfO]-ethylene glycol mixtures is shown in Figure 4.2a. The broad intensity in high frequency region, 3200-3600 cm^{-1}, reveals the typical stretching mode of the -NH and -OH site coming from the protic ionic liquids' cation and ethylene glycol, respectively. This figure

shows that the -OH vibration frequency shifts to lower wavenumber (red shift) as ethylene glycol mole fraction increases. In line with this finding, the chemical shift of -OH and -NH in ^{1}H NMR also shifted with increasing ethylene glycol composition. To understand the cation-anion interaction during ethylene glycol addition, Raman spectra were analysed to investigate the state of TfO^-, in particular in the range of ≈1033 cm^{-1}, attributed to the S-O stretching mode, where this mode is sensitive to local interaction. Fig 4.2c shows that the wavenumber shift from higher number to lower number upon ethylene glycol addition, which means that the local coordination between Im^+ and TfO^- was altered.

The investigation of protic ionic liquids series molecular interaction in Paper II, [HC_nIm][TFSI], was examined by the use of infrared and Raman. The interesting site, -NH stretching mode, was found in high frequency region (3255-3270 cm^{-1}) in the infrared spectra, Fig 4.2b. From this result, we can conclude that varying the alkyl chain length does affect the N-H frequency, which falls to lower frequency. This indicates, the longer the alkyl chain length, the stronger the hydrogen bond between Im^+-$TFSI^-$. It is interesting to note that the red shift increases up to n = 6 with less pronounce changes for alkyl chain longer than hexyl. However different observation obtained from Raman spectroscopy. Figure 4.2d shows peak fit analysis results of the most intense peak at ≈743 cm^{-1}. This region is a signature of the symmetric bending modes of the CF_3 group and sensitive to the strength of interaction with the chemical surrounding. The results indicates that there is no significant dependence of this frequency with alkyl chain length (n).

4.3 Nanostructuration

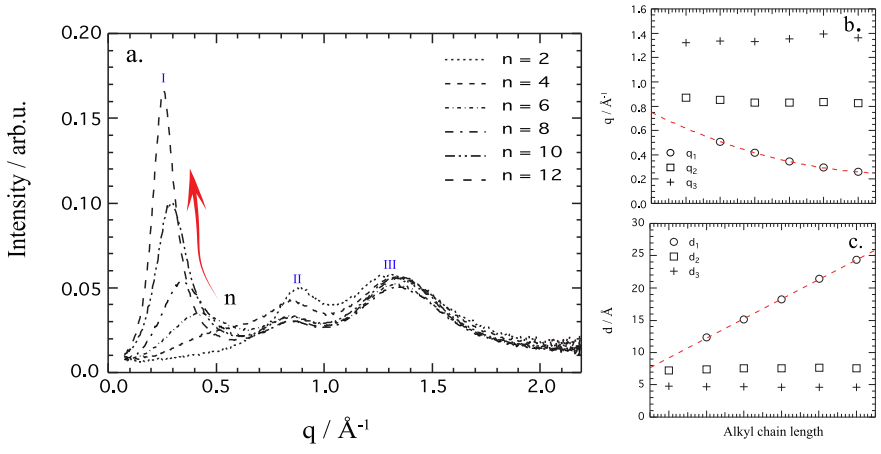

Figure 4.3: Wide angle X-ray scattering recorded spectra and analysis results for the [HC_nIm][TFSI] series, n from 2 to 12

The nanostructure of [C_nHIm][TFSI] series with alkyl chain length varying from

n=2 to n=12, in paper II, was elucidated from the obtained data by WAXS experiment. Fig 4.3 shows the scattering pattern of [C_nHIm][TFSI], n: 2-12. Three noticeable peaks were observed, where the first peak fall in the low q-range 0.2-0.6 Å (peak I or pre-peak), the second peak in the q-range 0.7-0.9 Å (peak II) and the third peak in the q-range 1.2-1.6 Å. Here we describe peak I or pre-peak is attributed to the separation distance between charged group by the alkyl chain attached on cation, while peak II is the characteristic of polar group distance of the same charge e.g anion-anion or cation-cation. These findings reveal that the nano-structure is found despite the liquid state and the short alkyl chains.

Further analysis in structural features of these protic ionic liquids series was performed to determine more precise peaks position and correlation distance. Peak fitting procedure was employed using Lorenztian function and cubic background. The scattering peak arising from the nonpolar domain of the cation (q_1) clearly show that the q-range shift to lower value as alkyl chain length increase this also verified by using Bragg's Law, $d_i = 2\pi/q_i$, the size of repeating distance clearly shifted to higher number as n increases in the case of d_1 where we attributed this as the repeating distance of the nonpolar domain. Therefore, it is important to note that the protic ionic liquid series in this study has shown the same behavior as the corresponding aprotic ionic liquid previously investigated [43, 58]. The fitting equation of the d_1 by linear regression is (Å) = 6.17 + 1.52 n, which means the correlation length with n is increasing 1.52 Å per CH_2 units. This value is smaller but still comparable to the previous finding by Martinelli et al.[58] and Russina et al [43].

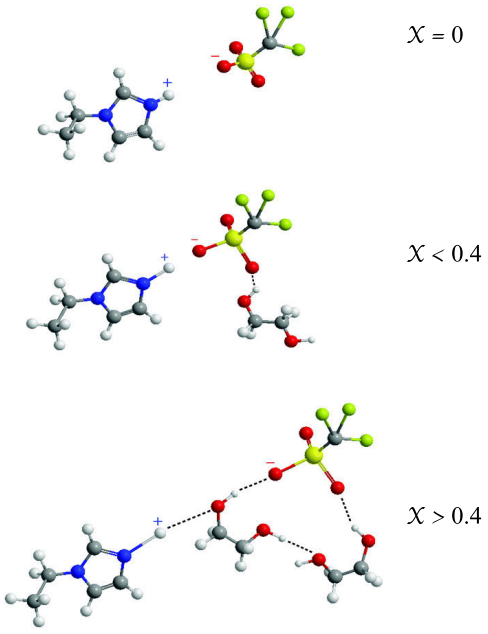

Figure 4.4: Proposed illustration of the possible H-bonds interactions in protic ionic liquid-ethylene glycol mixtures

4.4 Ionic mobility

The ionic mobility, i.e. self-diffusion coefficient of proton and cation of a protic ionic liquids reported in thesis was obtained by employing PFG-NMR experiments at ambient temperature. In the case of paper I, the diffusion of ethylene glycol was also measured, the molecular size of ethylene glycol smaller than the protic ionic liquid thus the ethylene glycol diffusion is faster than the protic ionic liquid. The self diffusion was investigated in the whole composition range of ethylene glycol, the present results show two distinct region. In mole fraction X < 0.4, the occurrence of Grotthuss mechanism is not observed, this might be due to the preferred interaction to anions. When X > 0.4 the D_{NH}/D_{cation} ratio increases, this explained by interposition of ethylene glycol to the cation-anion interaction, resulting stronger hydrogen bond and faster local dynamics as illustrated in Fig 4.4. To conclude, the excess composition of ethylene glycol can induce proton decoupled from its host molecules.

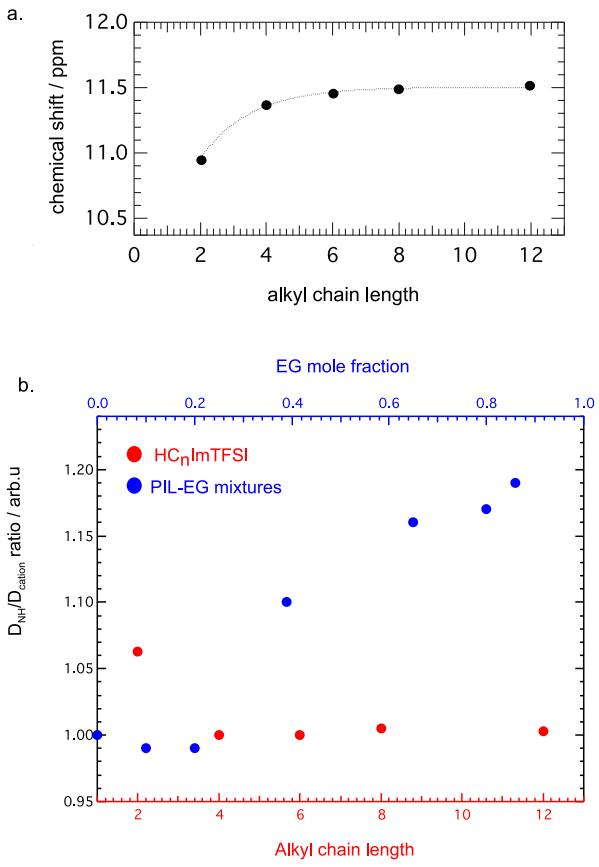

Figure 4.5: a) ^{1}H NMR results of [HC_nIm][TFSI] protic ionic liquids as a function of alkyl chain length, dashed line are simply guide to the eye; b) D_{NH}/D_{cation} ratio results of [C_2HIm][TfO]-ethylene glycol mixture and [HC_nIm][TFSI], varying n from 2 to 12

The -NH chemical shift as a function of alkyl chain are reported in Fig 4.5a. The figure shows that increasing the alkyl chain length lead the -NH chemical shift moving from 10.99 to 11.51 ppm. This is an indication that the hydrogen bond strength increases as n increasing with less changes for alkyl chain above hexyl. We hypothesised that stronger hydrogen bond obtained by increasing alkyl chain length, can exhibit proton motion decoupled from the imidazolium cation. This can be observed by D_{NH}/D_{cation} ratio significantly higher than one. To prove this PFG-NMR was employed and the results are depicted in Fig 4.5b, it is clearly seen that the self-diffusion ratio of proton and cation is not significantly higher than one ($D_{NH}/D_{cation} \approx 1$). Which means that despite longer N-H bonds are established in the case of cations with longer alkyl chains, this is not enough to induce a decoupled, or Grotthuss type, motion of the exchangeable protons.

4.5 Ionic conductivity

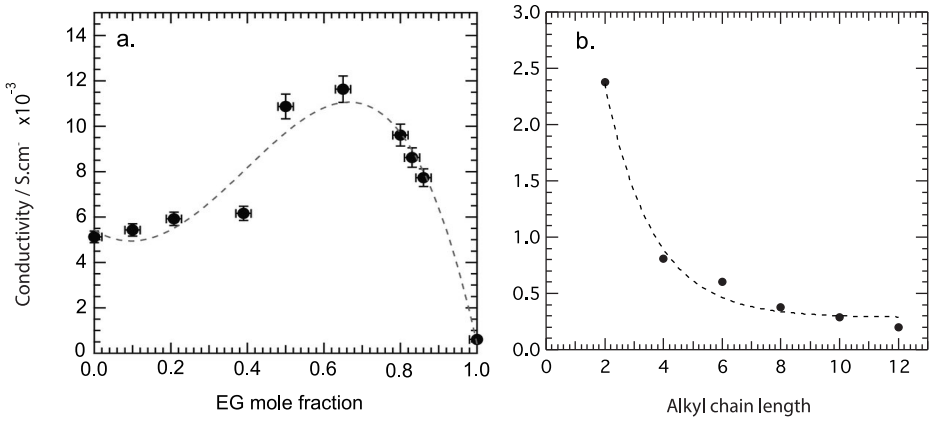

Figure 4.6: Ionic conductivity results of a) [C_2HIm][TfO]-ethylene glycol mixture and b) [HC_nIm][TFSI] protic ionic liquids, with n from 2 to 12. The dash line is simply a guide to the eye

Figure 4.6a displays the ionic conductivity measurements results of C_2HImTfO-ethylene glycol mixtures at 30 °C, ranging from 0 to 1 mole fraction of ethylene glycol . Upon the addition of ethylene glycol from 0 to 0.4 mol fraction, the ionic conductivity curve increases slightly. However, above $x > 0.4$, the conductivity value increases significantly and reached maximum peak at $x = 0.66$ then decreasing as the ethylene glycol composition > 0.8. This behavior is similar to the previous studies on imidazolium ionic liquids mixtures with ethanol and water by Rilo et al [59].

The conductivity of HC_nImTFSI series was investigated at temperature range -60 to 250 °C under nitrogen gas atmosphere. Figure 4.6b shows the conductivity of HC_nImTFSI at 25 °C as a function of alkyl chain length. The ionic conductivity is

monotonically decreasing as a function of n, a possible explanation of this behavior is that the viscosity increases as the consequences of the stronger hydrogen bond and lengthening the alkyl chain.

5 Conclusions and outlook

This thesis is focused on exploring the potential of protic ionic liquids as electrolytes for use in next generation proton exchange membrane fuel cells. The proposed protic ionic liquids have to fulfil several prerequisites, such as high decomposition temperature and high ionic conductivity. In order to design and obtain the desired protic ionic liquids, it is necessary to thoroughly understand the intermolecular interactions and the local dynamics. Two different approaches are proposed to modify the transport properties of protic ionic liquids; the first being mixing the protic ionic liquid with ethylene glycol, and the second being the modification of the cation's molecular structure. The whole work presented in this thesis is limited to protic ionic liquids based on the imidazolium cation.

In both approaches, the protic ionic liquids have been characterized by using ^{1}H NMR, diffusion NMR and vibrational spectroscopy. Summarising the results obtained from the binary mixture study (paper I), the cation and proton diffusion are dependent on the amount of ethylene glycol added to the mixture. If the mole fraction of ethylene glycol is higher than 0.4, the self-diffusion of the exchangeable proton is higher than that of the cation, which is a first indication of the Grotthuss mechanism. Ethylene glycol tends to interact with both cations and anions forming stronger intra- and inter-molecular hydrogen bonds. In the second study of this thesis (paper II), we find that the effect of extending the alkyl chain anchored to the cation is an elongation of the of the N-H bond (evidences from ^{1}H NMR and infrared spectroscopy) and a reduced ionic conductivity. These results indicate that modifications in the molecular structure of the cation affect the strength of hydrogen bonds, which in turn change mainly when varying the chain from the ethyl (n=2) to the hexyl (n=6). Longer chains do not result in further changes, as also observed for other properties such as nano-structuration (shown by X-ray scattering) and cation-anion interactions (revealed by Raman spectroscopy). Results from X-ray scattering reveal a certain degree of nano-structuration also for relatively short chains, as well as a local structure equivalent to that observed in analogous aprotic ionic liquids.

The overall results obtained from the two papers suggest some future directions of research. One aspect that could be investigated is the mixture of two (or more) protic ionic liquids, keeping either the cation or the anion the same. This type of liquid mixtures has been investigated for some aprotic ionic liquids, but only for a very few limited cases of protic cationic structures. The hypothesis is that the local interactions are strongly influenced by composition, with consequent effects also

on the thermal stability of the mixture. Understanding the nature and strength of hydrogen bonds will be at focus also in these studies. Another aspect to investigate in future works is how the local structure and dynamics vary when exchanging the imidazolium cation for a triazolium based structure. Triazolium based protic ionic liquids are not commercially available yet and will have to be synthesized in the lab. Compared to imidazolium, the triazolium cation possesses additional nitrogen sites able to act as hydrogen bond acceptor sites, hence possibly promoting the Grotthuss mechanism of proton hopping. Related questions will be the type of cation-anion coordination (the triflate and the bis(trifluoromethylsulfonyl)imide anions being first suitable candidates) as well as the effect of further structural modifications (for instance changes in the alkyl chain anchored to the cation). Finally, the effect of purity has been underestimated in the field of ionic liquids during the years, wherefore future efforts should be dedicated to finding more reliable analytical methods to quantify on one hand the real amount of undesired neutral species in the protic ionic liquid and on the other hand the degree of proton transfer which is directly connected to the ionicity of the liquid. In fact, recent studies indicate that molecular impurities and non-equimolar stoichiometries do influence dynamical and thermal properties.

References

[1] K. R. S. Robin D. Rogers, "Ionic Liquids–Solvents of the Future?", *Science*, 2003, **302**, 792–793.

[2] A. I. Siriwardana, in, ed. A. A. J. Torriero, Springer International Publishing, 2015, ch. Industrial Applications of Ionic Liquids, pp. 563–603.

[3] M. Palacio and B. Bhushan, "A Review of Ionic Liquids for Green Molecular Lubrication in Nanotechnology", *Tribology Letters*, 2010, **40**, 247–268.

[4] A. P. Abbott, G. Frisch, J. Hartley and K. S. Ryder, "Processing of metals and metal oxides using ionic liquids", *Green Chemistry*, 2011, **13**, 472–481.

[5] T. Welton, "Ionic liquids in catalysis", *Coordination Chemistry Reviews*, 2004, **248**, 2459–2477.

[6] T. L. Greaves and C. J. Drummond, "Protic Ionic Liquids: Properties and Applications", *Chemical Reviews*, 2008, **108**, 206–237.

[7] I. Staffell, D. Scamman, A. Velazquez Abad, P. Balcombe, P. E. Dodds, P. Ekins, N. Shah and K. R. Ward, "The role of hydrogen and fuel cells in the global energy system", *Energy Environ. Sci.*, 2019, **12**, 463–491.

[8] C. Mitsakou et al., "Environmental public health risks in European metropolitan areas within the EURO-HEALTHY project", *Science of The Total Environment*, 2019, **658**, 1630 –1639.

[9] D. R. MacFarlane, N. Tachikawa, M. Forsyth, J. M. Pringle, P. C. Howlett, G. D. Elliott, J. H. Davis, M. Watanabe, P. Simon and C. A. Angell, "Energy applications of ionic liquids", *Energy & Environmental Science*, 2014, **7**, 232–250.

[10] R. P. O'Hayre, *Fuel cell fundamentals.* Wiley, 2009.

[11] J. Wang, H. Wang and Y. Fan, "Techno-Economic Challenges of Fuel Cell Commercialization", *Engineering*, 2018, **4**, 352 –360.

[12] Y. Wang, D. F. R. Diaz, K. S. Chen, Z. Wang and X. C. Adroher, "Materials, technological status, and fundamentals of PEM fuel cells – A review", *Materials Today*, 2020, **32**, 178 –203.

[13] R. Rosli, A. Sulong, W. Daud, M. Zulkifley, T. Husaini, M. Rosli, E. Majlan and M. Haque, "A review of high-temperature proton exchange membrane fuel cell (HT-PEMFC) system", *International Journal of Hydrogen Energy*, 2017, **42**, Special Issue on Sustainable Fuel Cell and Hydrogen Technologies: The 5th International Conference on Fuel Cell and Hydrogen Technology (ICFCHT 2015), 1-3 September 2015, Kuala Lumpur, Malaysia, 9293 –9314.

[14] J. O. Jensen, D. Aili, Y. Hu, L. N. Cleemann and Q. Li, in *Nanocarbons for Energy Conversion: Supramolecular Approaches*, ed. N. Nakashima, Springer International Publishing, Cham, 2019, pp. 45–79.

[15] F. M. Collette, C. Lorentz, G. Gebel and F. Thominette, "Hygrothermal aging of Nafion®", *Journal of Membrane Science*, 2009, **330**, 21–29.

[16] A. Kusoglu and A. Z. Weber, "New Insights into Perfluorinated Sulfonic-Acid Ionomers", *Chemical Reviews*, 2017, **117**, 987–1104.

[17] M. B. Karimi, F. Mohammadi and K. Hooshyari, "Recent approaches to improve Nafion performance for fuel cell applications: A review", *International Journal of Hydrogen Energy*, 2019, **44**, 28919–28938.

[18] A. Chandan, M. Hattenberger, A. El-kharouf, S. Du, A. Dhir, V. Self, B. G. Pollet, A. Ingram and W. Bujalski, "High temperature (HT) polymer electrolyte membrane fuel cells (PEMFC) –A review", *Journal of Power Sources*, 2013, **231**, 264–278.

[19] M. B. Karimi, F. Mohammadi and K. Hooshyari, "Recent approaches to improve Nafion performance for fuel cell applications: A review", *International Journal of Hydrogen Energy*, 2019, **44**, 28919 –28938.

[20] N. Yaghini, L. Nordstierna and A. Martinelli, "Effect of water on the transport properties of protic and aprotic imidazolium ionic liquids – an analysis of self-diffusivity, conductivity, and proton exchange mechanism", *Phys. Chem. Chem. Phys.*, 2014, **16**, 9266–9275.

[21] N. Yaghini, V. Gómez-González, L. M. Varela and A. Martinelli, "Structural origin of proton mobility in a protic ionic liquid/imidazole mixture: insights from computational and experimental results", *Phys. Chem. Chem. Phys.*, 2016, **18**, 23195–23206.

[22] M. Campetella, M. Macchiagodena, L. Gontrani and B. Kirchner, "Effect of alkyl chain length in protic ionic liquids: an AIMD perspective", *Molecular Physics*, 2017, **115**, 1582–1589.

[23] C. Austen Angell, Y. Ansari and Z. Zhao, "Ionic Liquids: Past, present and future", *Faraday Discussions*, 2012, **154**, 9–27.

[24] J. S. Wilkes, "A short history of ionic liquids—from molten salts to neoteric solvents", *Green Chemistry*, 2002, **4**, 73–80.

[25] T. Welton, "Ionic liquids: a brief history", *Biophysical reviews*, 2018, **10**, 691–706.

[26] N. V. Plechkova and K. R. Seddon, "Applications of ionic liquids in the chemical industry", *Chemical Society Reviews*, 2008, **37**, 123–150.

[27] J. S. Wilkes and M. J. Zaworotko, "Air and water stable 1-ethyl-3-methylimidazolium based ionic liquids", *Journal of the Chemical Society, Chemical Communications*, 1992, 965–967.

[28] M. Taha, M. R. Almeida, F. A. e. Silva, P. Domingues, S. P. M. Ventura, J. A. P. Coutinho and M. G. Freire, "Novel Biocompatible and Self-buffering Ionic Liquids for Biopharmaceutical Applications", *Chemistry –A European Journal*, 2015, **21**, 4781–4788.

[29] R. Giernoth, "Task-Specific Ionic Liquids", *Angewandte Chemie International Edition*, 2010, **49**, 2834–2839.

[30] A. S. Amarasekara, "Acidic Ionic Liquids", *Chemical Reviews*, 2016, **116**, 6133–6183.

[31] P. A. Hunt, C. R. Ashworth and R. P. Matthews, "Hydrogen bonding in ionic liquids", *Chemical Society Reviews*, 2015, **44**, 1257–1288.

[32] H. Watanabe, H. Doi, S. Saito, M. Matsugami, K. Fujii, R. Kanzaki, Y. Kameda and Y. Umebayashi, "Hydrogen bond in imidazolium based protic and aprotic ionic liquids", *Journal of Molecular Liquids*, 2016, **217**, 35–42.

[33] J. Stoimenovski, E. I. Izgorodina and D. R. MacFarlane, "Ionicity and proton transfer in protic ionic liquids", *Physical Chemistry Chemical Physics*, 2010, **12**, 10341–10347.

[34] M. Yoshizawa, W. Xu and C. A. Angell, "Ionic Liquids by Proton Transfer: Vapor Pressure, Conductivity, and the Relevance of Î"pKa from Aqueous Solutions", *Journal of the American Chemical Society*, 2003, **125**, 15411–15419.

[35] M. B. Herath, T. Hickman, S. E. Creager and D. D. DesMarteau, "A new fluorinated anion for room-temperature ionic liquids", *Journal of Fluorine Chemistry*, 2011, **132**, 52–56.

[36] C. Maton, N. De Vos and C. V. Stevens, "Ionic liquid thermal stabilities: decomposition mechanisms and analysis tools", *Chemical Society Reviews*, 2013, **42**, 5963–5977.

[37] Y. Chen and T. Mu, in *Encyclopedia of Ionic Liquids*, ed. S. Zhang, Springer Singapore, Singapore, 2019, pp. 1–13.

[38] M. Kohagen, M. Brehm, Y. Lingscheid, R. Giernoth, J. Sangoro, F. Kremer, S. Naumov, C. Iacob, J. Kärger, R. Valiullin and B. Kirchner, "How Hydrogen Bonds Influence the Mobility of Imidazolium-Based Ionic Liquids. A Combined Theoretical and Experimental Study of 1-n-Butyl-3-methylimidazolium Bromide", *The Journal of Physical Chemistry B*, 2011, **115**, 15280–15288.

[39] N. Yaghini, L. Nordstierna and A. Martinelli, "Effect of water on the transport properties of protic and aprotic imidazolium ionic liquids –an analysis of self-diffusivity, conductivity, and proton exchange mechanism", *Physical Chemistry Chemical Physics*, 2014, **16**, 9266–9275.

[40] P. A. Hunt, "Quantum Chemical Modeling of Hydrogen Bonding in Ionic Liquids", *Topics in Current Chemistry*, 2017, **375**, 59.

[41] R. Hayes, G. G. Warr and R. Atkin, "Structure and Nanostructure in Ionic Liquids", *Chemical Reviews*, 2015, **115**, 6357–6426.

[42] T. L. Greaves and C. J. Drummond, "Solvent nanostructure, the solvophobic effect and amphiphile self-assembly in ionic liquids", *Chemical Society Reviews*, 2013, **42**, 1096–1120.

[43] O. Russina, A. Triolo, L. Gontrani, R. Caminiti, D. Xiao, L. G. Hines Jr, R. A. Bartsch, E. L. Quitevis, N. Pleckhova and K. R. Seddon, "Morphology and intermolecular dynamics of 1-alkyl-3-methylimidazolium bis(trifluoromethane)sulfonylamide ionic liquids: structural and dynamic evidence of nanoscale segregation", 2009, **21**, 424121.

[44] T. L. Greaves, A. Weerawardena, C. Fong, I. Krodkiewska and C. J. Drummond, "Protic Ionic Liquids: Solvents with Tunable Phase Behavior and Physicochemical Properties", *The Journal of Physical Chemistry B*, 2006, **110**, 22479–22487.

[45] M. A.B. H. Susan, A. Noda and M. Watanabe, in *Electrochemical Aspects of Ionic Liquids*, ed. H. Ohno, Wiley, 2005, ch. 5.

[46] K.-D. Kreuer, "Proton Conductivity: Materials and Applications", *Chemistry of Materials*, 1996, **8**, 610–641.

[47] A. Noda, M. A.B. H. Susan, K. Kudo, S. Mitsushima, K. Hayamizu and M. Watanabe, "Brønsted Acid-Base Ionic Liquids as Proton-Conducting Nonaqueous Electrolytes", *The Journal of Physical Chemistry B*, 2003, **107**, 4024–4033.

[48] *Principles and Applications of Thermal Analysis*, ed. P. Gabbott, Blackwell Publishing Ltd, 2008.

[49] M. Wagner, in *Thermal Analysis in Practice - Fundamental Aspects*, Hanser Publishers.

[50] W Wagner and K. R, "Densimeters for very accurate density measurements of fluids over large ranges of temperature, pressure, and density", *Metrologia*, 2004, **41**, S24–S39.

[51] *U-tube technology in digital laboratory density meters*, Anton Paar GmbH, `https://wiki.anton-paar.com/en/u-tube-technology-in-digital-laboratory-density-meters/`.

[52] N. Osswald, Tim Rudolph, in, Hanser Publishers, 2015, ch. 1.2.

[53] K. Walters and W. Jones, in *Instrumentation Reference Book (Fourth Edition)*, ed. W. Boyes, Butterworth-Heinemann, Boston, Fourth Edition, 2010, pp. 69–75.

[54] A. Y. Malkin and A. Isayev, in *Rheology - Concept, Methods, and Applications*, ChemTec Publishing, 2017, pp. 265–375.

[55] E. O. Stejskal and J. E. Tanner, "Spin Diffusion Measurements: Spin Echoes in the Presence of a Time Dependent Field Gradient", *The Journal of Chemical Physics*, 1965, **42**, 288–292.

[56] J. G. Huddleston, A. E. Visser, W. M. Reichert, H. D. Willauer, G. A. Broker and R. D. Rogers, "Characterization and comparison of hydrophilic and hydrophobic room temperature ionic liquids incorporating the imidazolium cation", *Green Chemistry*, 2001, **3**, 156–164.

[57] M. C. Kroon, W. Buijs, C. J. Peters and G.-J. Witkamp, "Quantum chemical aided prediction of the thermal decomposition mechanisms and temperatures of ionic liquids", *Thermochimica Acta*, 2007, **465**, 40–47.

[58] A. Martinelli, M. Maréchal, Å. Östlund and J. Cambedouzou, "Insights into the interplay between molecular structure and diffusional motion in 1-alkyl-3-methylimidazolium ionic liquids: a combined PFG NMR and X-ray scattering study", *Physical Chemistry Chemical Physics*, 2013, **15**, 5510–5517.

[59] E. Rilo, J. Vila, S. García-Garabal, L. M. Varela and O. Cabeza, "Electrical Conductivity of Seven Binary Systems Containing 1-Ethyl-3-methyl Imidazolium Alkyl Sulfate Ionic Liquids with Water or Ethanol at Four Temperatures", *The Journal of Physical Chemistry B*, 2013, **117**, 1411–1418.